NASA

Technical Memorandum 79572

Scattering of Terrestrial Kilometric Radiation at Very High Altitudes

J. K. Alexander
M. L. Kaiser
P. Rodriguez

June 1978

National Aeronautics and
Space Administration

Goddard Space Flight Center
Greenbelt, Maryland 20771

SCATTERING OF TERRESTRIAL KILOMETRIC RADIATION AT VERY HIGH ALTITUDES

by

J. K. Alexander, M. L. Kaiser, and P. Rodriguez
Planetary Magnetospheres Branch
Laboratory for Extraterrestrial Physics
Goddard Space Flight Center
Greenbelt, MD 20771

ABSTRACT

On a number of occasions during the 3.8-yr. operating lifetime of RAE-2, we observed strong terrestrial kilometric radiation when the spacecraft was over the far side of the moon and when the low altitude terrestrial magnetosphere was completely obscured from view. If these deep lunar occultation events are used to infer radio source locations, then we find that the apparent source must sometimes be situated at geocentric distances of 10 to 40 R_E or more. From an analysis of these events, we show that they are probably due to propagation effects rather than the actual generation of the emission at such large distances. The kilometric radiation can be generated near the Earth at auroral latitudes and subsequently strongly scattered in the magnetosheath and nearby solar wind to produce the large apparent distances. The most likely scatterers are density inhomogenieties in the magnetosheath plasma and ion plasma waves in the magnetosheath and the upstream solar wind.

SCATTERING OF TERRESTRIAL KILOMETRIC RADIATION AT VERY HIGH ALTITUDES

INTRODUCTION

Abundant evidence now exists that one of the most common and persistent manifestations of magnetospheric substorms is the generation of intense kilometer wavelength radio emissions. Recent satellite studies of these emissions have shown that in many cases the radiation source must be located on "auroral" field lines at a geocentric radial distance of about 2-4 R_E, and that they occur most frequently over the evening local time sector in close association with discrete auroral arcs and enhancements in the auroral electrojet. For these reasons, the emissions have been named "auroral kilometric radiation" (AKR) by Kurth et al. (1975). In earlier papers we showed that two-dimensional source position projections obtained from lunar orbit indicated that there are also a significant number of cases with much larger source altitudes (Kaiser and Alexander, 1976; Alexander and Kaiser, 1976). In fact, some observations of emissions emanating from the dayside hemisphere appeared to suggest that the radiation might even be generated in the outer regions of the dayside magnetosphere and perhaps even in the vicinity of the magnetosheath (Alexander and Kaiser, 1977). Until the connection or distinction between the emissions over such an apparently wide altitude range is understood we have continued to use the more general term "terrestrial kilometric radiation" (TKR).

The observations of kilometric emissions at such very large distances from the Earth have presented a particularly perplexing problem. Dynamic spectral measurements show that the distant emissions must be closely related to the near-Earth AKR as part of the same radiation phenomenon.

However, it is difficult to conceive of a single emission mechanism that can account for the generation of radiation over such a wide distance range, especially since the radiation frequencies of the distant "sources" are substantially higher than the characteristic frequencies of the plasma in the outer magnetosphere. An alternative to having the radiation actually generated at the very large distances is to suppose that this class of events is due to radiation created in a lower altitude source region which is subsequently scattered or reflected off inhomogeneities which occur in a limited region of space and which lead to apparent sources in the outer magnetosphere (Kaiser and Alexander, 1977).

In this paper we examine the latter hyopthesis in order to interpret what may be the most remarkable members of the group of distant kilometric emissions - namely those events with apparent source distances of greater than 10 R_E. The primary source of data for this study is the 3.5-yr, collection of lunar occultation measurements obtained by the Radio-Astronomy-Explorer-2 satellite. We have reviewed the entire series of RAE observations in order to identify and analyze those occultation events in which we detect significant TKR when the Earth is more than 10^o below the moon's limb corresponding to projected geocentric radial distances of greater than 10 R_E for the apparent radio source. In subsequent sections we will illustrate the characteristics that are common to this group of events and will show how the radiation appears to come from near or beyond the outer boundaries of the magnetosphere. Finally, we will examine the plausability of irregular refraction or scattering as an alternative

to the generation of the emission in these regions and will discuss the implications of this hyopthesis for studies of the solar wind-magnetosphere interface.

OBSERVATIONS OF THE DISTANT RADIATION

The technique of using RAE-2 lunar occultations to determine source positions has been described in detail by Alexander and Kaiser (1976). Basically, the Earth is obscured from view on a portion of each 222-min orbit of the moon for a period of about 7 days every two weeks. The angular diameter of the moon as viewed from the 1100-km altitude of RAE is 76°, and the maximum duration of deep (i.e., central) occultations of the Earth is 48 min. Since the angular size of the Earth as seen from the lunar distance is about 2°, the entire magnetosphere inside a radial distance of 38 R_E can be blocked from view when RAE is on the opposite side of the moon from the Earth. Radio source positions are generally determined by noting the times of disappearance and reappearance of emissions during an occultation and then calculating the direction corresponding to the position of the intersection of the projection of the moon's limb at those two times. The ambiguity due to the fact that two such intersection points always exist is resolved by making the (usually) reasonable assumption that the limb intersection point nearest to the Earth is the most probable source location. When emission is observed even during very deep occultations this assumption cannot necessarily be made, and we can only put estimated limits on the direction and radial distance of the source.

The dynamic spectra in Figure 1 illustrate the detection of TKR when the Earth was more than 10° below the lunar horizon. Each of the six panels display data obtained with a 32-channel receiver during

a 100-min. period centered on an occultation of the Earth. The predicted times of the geometric occultation of the planetary disk are indicated by the arrows on top of each panel. Notice that in the high frequency channels above 4 MHz the noise levels due to man-made signals from the surface of the Earth are cut off precisely at the geometrical occultation times. The dominant feature of all of these examples is the strong TKR which often reaches receiver saturation level intensity at frequencies near $\sim$ 250 kHz outside of the occultation period and which persists to some extent even at mid-occultation at frequencies around 150 kHz. On some occasions (such as 1506-1514 U.T. on March 19, 1976) there is a brief "bite" out of the emission indicating that the apparent source region was completely obscured for a short interval, but in other cases relatively strong emission was detected at all times.

The appearance of the dynamic spectra during these events provides compelling evidence that the noise bands that persist deep into the occultation must have a terrestrial (i.e., magnetospheric) origin. Although we have considered the possibility of alternative sources, our previous studies with the RAE and IMP-6 radio astronomy experiments have identified no other comparable sources in this frequency range. Solar radio bursts exhibit very distinctive and quite different dynamic spectral signatures. We sometimes detect strong plasma wave emissions at the interplanetary electron plasma frequency and its first harmonic, but those events appear as very narrow lines. (For example, note Jan. 11, 1976 at 50 and 100 kHz in Figure 1.) The nonthermal continuum radiation described by Gurnett (1975) is considerably weaker and also has a different spectral shape. We see no alternative to concluding that these events correspond to the reception by RAE of low frequency TKR

from geocentric distances that are so large as not to be occulted by the moon.

The large distances implied by these events are illustrated in Figure 2 where we show two examples of the average power flux density spectrum observed during the middle of an Earth occultation (left panel) and the projection of the lunar limb relative to the position of the Earth as a function of time (right panel). For the case of Figure 2a (corresponding to the top panel in Figure 1) there is a peak at 110 kHz in the average spectrum between 0330 and 0340 U.T. A closer examination of the detailed data at 110 kHz shows a sharp drop in the flux between 0337 and 0342 U.T. that probably corresponds to occultation of the 110 kHz emission region. The apparent source location inferred from those disappearance and reappearance times is indicated in the right-hand panel of Figure 2a. The corresponding projected radial distance for the 110 kHz is $\sim 22\ R_E$. On the other hand, the more intense 250 kHz emission in the center of the TKR frequency band disappears and returns almost in coincidence with the disk of the Earth, and so the 250 kHz source appears to be located very near the Earth at a projected altitude of less than $1\ R_E$. Therefore this event suggests that although the most intense radiation at frequencies near 250 kHz probably came from a source near the Earth, there was a significant fraction of the radiation at frequencies near 100 kHz that arrived along a line of sight that would not even intercept the nominal magnetosphere.

The example illustrated in Figure 2b gives a similar result. An intense 250 kHz source appeared to be situated relatively close to the Earth at a projected goecentric distance of $6.5\ R_E$. However strong

emission centered near 110 kHz persisted throughout the occultation period so that there was no clear evidence of even a brief obscuration of the low frequency source. As the right-hand panel of Figure 2b indicates, a portion of the apparent 110 kHz source must be at a projected geocentric distance of greater than 27 R_E.

On at least six occasions we observed strong TKR activity throughout the entire span of a central occultation of the Earth, and the circumstances for those events are shown in Figure 3. For each event the shaded region denotes the area that was completely blocked from view at the mid-point of the occultation when TKR was still detected. The frequency of peak flux density at that time is indicated by f_o. During these events the observed radiation had to arrive from a direction outside the shaded fans. For these special cases, the most plausible source location would appear to be a region relatively close to RAE such as the nearby solar wind or magnetosheath. We have identified at least 80 events of the type illustrated in Figure 1 and 2 between June 1973 and April 1977 where clear ($\geq$10 dB above background) TKR was observed when the Earth was at least 10^o below the lunar horizon.

On at least 21 occasions included in the catalog of 80 peculiar occultations a brief, essentially complete bite in the TKR could be detected, and for those events we have been able to infer source position estimates by the occultation timing/limb intersection technique discussed above. The results of that analysis are shown in Figure 4. Each arrow represents the line of sight from RAE-2 to the apparent TKR source as derived from the occultation data and rotated into the

ecliptic plane. Also shown for reference are the average positions of the bow shock and the magnetopause as derived by Fairfield (1971). The most interesting aspect of the results in Figure 4, when taken together, is the fact that they provide strong evidence that the radiation comes from the magnetosheath. When the source direction lines are extended so that we can use triangulation to estimate the most probable source location we find the intersections of sight lines highly concentrated in the region of the nominal magnetosheath. The region inside the magnetopause tends to be a region of avoidance. The bow shock and the upstream solar wind cannot be absolutely ruled out as source regions, and we shall return to this point shortly.

When we compare the catalog of 80 peculiar occultation events to the average occurrence morphology of TKR there is no evidence to suggest that these events correspond to particularly unusual radio storms. The auroral electrojet index was at substorm levels (AE > 200 γ) for more than 80% of the cases. However, TKR is known to occur preferentially during periods of high AE (Voots et al., 1977; Kaiser and Alexander, 1977), and the average value of AE for these events was not significantly greater than the average AE for all TKR. Similarly, the North-South component of the interplanetary magnetic field was southward ($B_z < 0$) for over 80% of the cases, but the general association between southward IMF and magnetospheric substorms is also well known.

On the other hand, we have found that at least two-thirds of the distant emission events occurred at the time of solar wind density enhancements associated with high speed streams, sector boundaries or noncompressive density enhancements (NCDE's). Gosling et al., (1977) have pointed out that NCDE's are characterized by density enhancements

which are not associated with compressions along the rising portions of high speed streams but which are observed when the solar wind velocity is relatively low and constant or is falling, for example, at the end of a period of high speed flow. Roughly 50% of the periods during which we observed the peculiar TKR occultations occurred during such conditions. Gosling et al. (1977) suggest that NCDE's may be highly structured volumes of gas due to slow-moving coronal mass ejections which are being carried along by the solar wind. Apparently these density events can stimulate the conditions in the magnetosheath or in the nearby solar wind which are necessary to cause the distant TKR events.

A second interesting pattern in the class of distant emissions concerns the frequency, f_o, at which we observe the peak power flux density during the deepest (i.e., most distant) part of the occultation. In Figure 5 we plot the value of f_o (as derived at mid-occultation from dynamic spectra similar to Figure 1 and flux spectra as in Figure 2) versus the hourly average solar wind electron plasma frequency (King, 1977). There is a direct relationship between the frequency range in which the distant TKR emissions are observed and the interplanetary plasma frequency. A linear least squares fit to the data in Figure 5 gives a slope of 3.84.

DISCUSSION

At this point we are presented with the following picture. There are occasions (roughly estimated to be $\geq$ 10% of the time) when a portion of the TKR observed by RAE-2 in lunar orbit clearly arrives from a large angular distance from the Earth. These events usually are observed in the low frequency half of the $\sim$ 400 kHz-wide TKR band and usually, but

not always, appear at a lower power flux density than that measured when the entire magnetospheric system is in the field of view. The lunar occultation measurements suggest that at times the relevant region must be at a geocentric distance of $\geq 38\ R_E$ and may even be as far from the Earth as the moon at $60\ R_E$. Two major questions still remain. First, is the radiation actually generated at these large distances or are these events only due to "apparent sources" that arise from a peculiar propagation effect? Second, what is the specific physical mechanism involved? We will examine these questions in the light of several lines of evidence below.

Generation In or Near the Magnetosheath

Plasma densities in the magnetosheath will tend to be enhanced over the solar wind densities and, on the average, will respond directly to the temporal variations in the solar wind density (and plasma frequency). Magnetohydrodynamic models of the solar wind-magnetosphere interaction (e.g., Spreiter and Rizzi, 1974) predict maximum enhancement in the density of about a factor of 4 immediately behind the nose of the bow shock and of factors of ~ 1 to 3 in the flanks of the magnetosheath. The corresponding enhanced electron plasma frequencies in the regions away from the subsolar point would tend to be 1 to 1.7 times the interplanetary values. Therefore if the distant TKR is due to radiation actually generated in the sheath region, then the peak power must be emitted at frequencies that are systematically higher than twice the plasma frequency of the most dense plasma along the flanks of the magnetosheath. Although it may be possible for such a mechanism to be effective at times, the fact that the dynamic spectra show that the

distant emissions form an integral part of a larger band of emission whose central frequencies appear to come from relatively close to the Earth argues against the generation of the low frequency emission at the distant locations.

Irregular Refraction Effects in the Magnetosheath

A somewhat more palatable explanation for the distant sources can be fashioned by considering scattering or refraction of low frequency waves in the magnetosheath. The index of refraction for a wave frequency of 100 kHz can differ significantly from unity in the magnetosheath, and, indeed, total internal reflection can occur at the magnetopause for incidence angles larger than about 60°. In order to estimate the amount of scattering of the low frequency TKR that might be caused by irregularities in the magnetosheath we use Chandrasekhar's (1957) statistical theory of the angular spreading of rays. The root mean square angular spread is given by

$$\phi_{rms} = \sqrt{\frac{\Delta S}{h_s}} \cdot \frac{\Delta N}{N} \cdot \pi^{1/4} \left(\frac{f_p}{\mu f}\right)^2 \text{ radians} \qquad (1)$$

where ΔS = the path length through the scattering medium, h_s = the irregularity scale size, N = the average electron density, ΔN = the rms fluctuation in electron density, f_p = the electron plasma frequency, f = the wave frequency, and μ = the index of refraction of the medium. When RAE is situated over the dusk meridian at 18 hr. local time the path length, ΔS, through the magnetosheath is typically $\sim 11\ R_E = 7 \times 10^4$ km. If we assume a density enhancement in the magnetosheath of 2x the solar wind density (Howe and Binsack, 1972) and recall from Figure 5

that $f_o \simeq 3.8\ f_{p(sw)}$, then

$$\frac{f_{p(ms)}}{f} = \frac{(2)^{1/2}}{3.8} \quad \text{and} \quad \mu = 0.93.$$

Then

$$\phi_{rms} = 2.7 \times 10^3\ (h_s)^{-1/2}\ (\Delta N/N), \tag{2}$$

where ϕ_{rms} is in degrees and h_s is in kilometers.

There is very little information available concerning the plasma density structure of the magnetosheath, and so our knowledge of the appropriate ranges for h_s and $\Delta N/N$ is correspondingly vague. In a scattering estimate very similar to ours, Vesecky and Frankel (1975) used values considered characteristic of the solar wind -- namely $h_s = 300$ km and $\Delta N/N = 0.05$. For that case we get $\phi_{rms} = 7.8^o$ in agreement with Vesecky and Frankel who predicted that ϕ_{rms} would be only a few degrees at ~ 100 kHz. More importantly, they pointed out that this would only be a lower limit estimate of the magnitude of the scattering since the magnetosheath plasma is likely to be more disturbed and inhomogeneous than the solar wind.

A better picture of the relevant structure of the magnetosheath might be derived from observations of large amplitude hydromagnetic waves discussed by Kaufmann and Horng (1971). They interpreted large amplitude magnetic field fluctuations observed in the 0.01 to 0.1 Hz frequency range as slow magnetoacoustic waves associated with plasma condensations having a scale size of ~ 1000 km. Using this scale size and assuming density fluctuations of 50%, we get $\phi_{rms} = 42^o$. Such

an rms scattering angle could easily produce the kind of results we have described earlier in this paper. We can not take the quantitative prediction for ϕ_{rms} too literally, because the expression in equation (1) only applies to the case of small angle scattering where individual deflections of a ray are small so that a statistical approach can be applied. The most important point is that if significant density fluctuations can occur in association with the magnetoacoustic waves discussed by Kaufmann and Horng and if these structures are common features in the disturbed magnetosheath, then we should expect strong scattering to occur for frequencies near 100 kHz. The magnetosheath would then appear as a relatively bright halo of irregularly refracted TKR in a manner similar to patches of fog illuminated by a street light.

In order to get a quantitative estimate of the amplitude of electron density fluctuations in the magnetosheath which might cause the scattering of the low frequency TKR we have examined data from the GSFC radio wave experiment on IMP-6. That experiment often detected narrow spectral lines at the ambient electron plasma frequency in both the solar wind and magnetosheath. Although these f_p emissions were less commonly observed when IMP-6 was in the magnetosheath than in the solar wind, there were a number of very clear cases when both the absolute value of the magnetosheath electron plasma frequency and its relative fluctuations could be measured unambiguously on time scales longer than 5 sec. A preliminary analysis of a sample of these data has shown a number of occasions in the dusk hemisphere magnetosheath where the rms density fluctuations ($\Delta N/N$) were are large as 30-40% and where the irregularity scale sizes (assuming a flow velocity of

~ 300 km/sec) where 20000 km. Very recent direct measurements of magnetosheath plasma by ISEE-1 agree with these estimates (J. Scudder, private communication). These results confirm the occurrence of the level of density fluctuations necessary to cause strong scattering of the TKR, but the inferred scale sizes are somewhat larger than the scattering model would predict.

In a test of the scattering hypothesis, we have compared the occurrence statistics for the catalog of 80 peculiar occultation events with a phenomenological model for magnetosheath propagation effects in Figure 6. The basic hypothesis is that the detection of scattered TKR when RAE was behind the moon would depend on the amount of TKR power incident on the magnetosheath and on the line of sight path length through the magnetosheath. In the upper panel in Figure 6 we have plotted the average power pattern for TKR at 110 kHz derived from all RAE data when the Earth was not occulted. This should be representative of the input power pattern to the proposed scattering medium as a function of position. In Figure 6b we show the minimum magnetosheath path length (i.e., along the direct line of sight to the Earth) for an observer in lunar orbit. These data are taken from the average magnetopause and bow shock locations derived by Fairfield (1971). We have multiplied the two local time distributions together in Figure 6c to derive a "predicted" occurrence distribution based on those two factors. This simplified model can then be compared directly with the actual observed event occurrence probability which is shown in the bottom panel of the figure (6d). The agreement between the two curves is remarkably good and lends support to the "propagation effect" hypothesis.

Bragg Scattering by Ion Waves

In contrast to the case discussed above involving irregular refraction by large scale inhomogeneities in the magnetosheath, we now consider the case of scattering by microscale structures along the TKR ray path. The observation of low frequency TKR when the Earth is as much as 38° below the lunar limb, implies that large angle scattering must occur to TKR waves, by at least 38° and sometimes through as much as 180° (back scattering). Such large deviations in propagation direction suggest that the scattering centers must interact strongly, i.e. coherently, with TKR waves. In such a scattering interaction the conservation relations $\vec{k} = \vec{k}_i - \vec{k}_s$ and $\omega = \omega_s - \omega_i$ apply to the incident (i) and scattered (s) wave vectors and frequencies, with the scattering center being characterized by k and ω. The scattering angle θ, measured with respect to the incident direction, is determined from the Bragg scattering formula (where $|\vec{k}_i| \sim |\vec{k}_s|$) $|\vec{k}| = 2\, k_i \sin(\theta/2)$. Thus, for large angle scattering $|\vec{k}| \sim k_i$ or the wavelength $\lambda = \lambda_i/2$. where $2\pi/\lambda = k$, For backscattering, $\theta = 180^{\circ}$ and $\vec{k} = 2\,\vec{k}_i$, or $\lambda = \lambda_i/2$. The fraction of incident power that is scattered is proportional to the spectrum of density fluctuations $S(\vec{k}, \omega)$, where $\vec{k}$ and ω refer to the normal modes of the plasma (Sheffield, 1975). In a stable plasma, the normal modes are ordinarily Landau damped and so have amplitudes which are consistent only with thermal fluctuations. Such waves are expected to have only minimal and random scattering interactions. However, in an unstable plasma, such as occurs when energetic charged particle beams interact with the thermal distribution, enhanced plasma wave amplitudes are generated so that $S(\vec{k}, \omega)$ can become very large. Strong scattering

is then possible when the Bragg condition is satisfied by the plasma waves and the incident electromagnetic waves.

Enhanced plasma wave turbulence commonly occurs in a large volume of the solar wind near the Earth's bow shock. A study of the beam-plasma interactions that result from the emission of energetic ions and electrons by the bow shock into the solar wind (Rodriguez, 1978b) has shown that the plasma waves required to produce strong scattering of TKR can occur in the solar wind and very likely also in the magneto-sheath. In particular, plasma waves correlated with energetic ions, which we will call ion waves, can have wavelengths on the order of (1-2) km and are thus closely matched to the range of scattered TKR wavelengths of (1.9-3.6) km, corresponding to the scattered TKR frequency band (83-155) kHz. Electron plasma oscillations, which are correlated with energetic electrons, may have wavelengths on the order of 1 km also, but appear to be less important for scattering, as will be discussed below.

The spectrum of solar wind plasma waves associated with energetic electrons and ions emitted by the bow shock is similar to the spectrum detected even more often (essentially always) in the magnetosheath (Rodriguez, 1978a). If ion waves in the magnetosheath can also be (1-2) km in wavelength, then a very large, permanent scattering region extends around the Earth which is easily within the radiation patterns of TKR from both north and south terrestrial poles. The source of plasma wave turbulence in the magnetosheath is not well established, but may be associated with energetic particles in the magnetosheath, such as the such as the energetic ions observed by West and Buck (1976).

The geometry that we hypothesize for large angle scattering of TKR by plasma waves in the solar wind and magnetosheath is depicted in Figure 7. The average location of the magnetopause and bow shock are shown along with a typical magnetic field direction in the ecliptic plane. The figure is similar to the actual geometry that occurred for the central occultation of December 14, 1973 illustrated in Figure 3. The shadow zone for the central occultation is shown as the shaded cone. The areas (actually volumes) identified as regions of plasma wave turbulence are determined by the vectoral addition of the solar wind convection velocity and the velocity vector of an energetic particle ($\sim$ 1 kev) outwardly emitted along the magnetic field direction. Typical boundary locations (dashed lines) for electrons and ions are discussed by Greenstadt (1976). As depicted in the figure, the emission cone for ion waves is generally symmetric about the magnetic field direction and fairly broad; a similiar emission cone occurs in the magnetosheath (Rodriguez, 1978a). Electron plasma oscillations also display a field-symmetric emission cone that is somewhat less broad (Rodriguez and Gurnett, 1975). Thus, for a given direction of an incident (i) TKR ray, there is available a broad range of plasma wave k-vector directions to satisfy the Bragg relation and scatter the ray (s) through a large enough angle θ to be detected behind the moon. Two rays are shown scattering simultaneously toward the moon, one from the solar wind and one from the magnetosheath. In fact, for the scattering mechanism that we are proposing the solar wind and magnetosheath are probably indistinguishable and a given observation of scattered TKR may result from rays coming from many, a few, or only one scattering

center. Scattering may actually be more probable from the magnetosheath because the plasma wave turbulence is always present there, while in the solar wind the location of the region of plasma wave turbulence is influenced by the orientation of the magnetic field.

A characteristic of the observation of scattered TKR is that only a lower frequency portion of the full TKR spectrum is scattered. The TKR band is typically 83-500 kHz (Kaiser and Alexander, 1977), while the scattered spectrum is about 83-155 kHz. This observation provides supportive evidence for plasma wave scattering. Rodriguez (1978b) has shown that the wavelength spectrum of solar wind ion waves appears to be broad enough to include the 1-2 km range. In Figure 8 we plot the Bragg relation in terms of the wavelength ratio, $\lambda/\lambda_i = (2 \sin \theta/2)^{-1}$, where λ is the plasma wave density fluctuation wavelength and λ_i is the incident TKR wavelength. With a range (1-2) km for λ and (1.9-3.6) km for λ_i it is clear that the Bragg formula predicts large angle scattering, $\theta \approx 60^\circ$ to 180°, which we have shown is necessary to explain the observations. For shorter TKR wavelengths, i.e., for frequencies above 155 kHz, the ratio λ/λ_i becomes large and the predicted scattering angle is small; thus high frequency TKR cannot be scattered through a large enough angle to be detected behind the moon.

The Bragg relation probably cannot apply strictly to large volumes of the solar wind or magnetosheath. The dimensions of a scattering center are difficult to estimate. Certainly a minimum size is on the order of several kilometers; however, a more characteristic size which can scatter appreciable power in a given direction would be determined by the distance and time scales over which energetic particle beams can

drive phase coherent, or approximately phase coherent, plasma waves. Such information is presently unknown.

The spectrum of electromagnetic waves scattered by plasma waves is observed at a frequency $\omega_s \sim \omega_i \pm \omega$, where ω is the frequency of the plasma wave. For ion waves, $\omega \leq 2\ \omega_{pi}$ therefore the ion wave frequency is fairly low since typically, $f_{pi} = \omega_{pi}/2\pi \sim 0.5$ kHz. TKR scattered by solar wind ion waves would thus show no detectable frequency shift, consistent with our observations. If electron plasma waves were strong scattering centers for TKR, a frequency shift of $f = \omega_{pe}/2\pi \sim 20\text{-}30$ kHz, where ω_{pe} is the electron plasma frequency, could be detected at TKR frequencies. We have no clear evidence of such frequency shifts in the scattered spectrum, and thus we conclude that for plasma wave scattering of TKR, ion waves must be the principal scattering centers. This conclusion is consistent with theory (Bekefi, 1966, p. 269), which shows that the cross section for ion wave scattering is much larger than for electron plasma oscillations.

In laboratory and ionospheric observations the scattering ion waves are identified as ion acoustic waves (Bekefi, 1966; Farley, 1971; Sheffield, 1975). As discussed in Rodriguez (1978b), we have refrained from identifying the ion waves we propose for TKR scattering centers as ion acoustic waves, although they may be similar. Ion acoustic waves in the solar wind have been discussed by Gurnett and Frank (1978), and shown to have a frequency spectrum similar to the beam-generated ion waves, but the wavelengths of the ion acoustic waves are about 0.1 km. Such waves cannot Bragg

scatter TKR, as indicated on Figure 8. It is possible that the ion waves are Buneman waves, which tend to saturate at a frequency of 1.75 ω_{pi} (Hamberger and Jancarik, 1972). The important characteristic of the waves for TKR scattering, however, is that they have the appropriate wavelength, and this appears to be possible.

An additional bit of evidence that seems to support the ion wave scattering hypothesis lies in the apparent association of TKR scattering with noncompressive density enhancements (NCDE's). Gosling et al. (1977) indicate that during NCDE events the electron and proton temperatures tend to decrease; the published examples of these events indicate however, that the ratio of the temperatures T_e/T_p tends to increase. An increase in T_e/T_p is conducive to enhanced ion wave turbulence, such as has been shown to be the case for the bow shock (Rodriguez and Gurnett, 1976), and we may therefore expect that TKR scattering off solar wind and magnetosheath ion waves may become more probable during NCDE's. Since the most intense ion wave turbulence generally occurs at the bow shock, we do not exclude the possibility that the bow shock by itself is an important scatterer of TKR.

Lunar Wake Refraction

For some occultations of the earth, RAE-2 passes through the lunar wake. On these occasions, the spacecraft passes through a region of changing density which can produce a substantial change in the index of refraction. The density variation across the lunar wake has been studied by Whang (1969) and Ness et al. (1968), and they show that the density quickly decreases to a near-void within about 0.5 R_m transverse to the axis of the wake. In order to estimate the angle of deviation that a TKR

ray would experience in the lunar wake, we shall assume that the density decreases to zero sharply at 1 R_m transverse to the wake axis. For a TKR frequency of 100 kHz and a typically high magnetosheath density of $N \sim 40$ cm^{-3}, the index of refraction outside the wake is 0.82. Inside, the wake, the index of refraction is nearly 1.0. Since the refractive index increases in the wake, a ray will tend to be refracted inward toward the wake axis. Assuming an angle of incidence of 60° such that the incident ray is within the shadow cone, the angle of the refracted ray is 45°. The angle of deviation is therefore 15°. Such a deviation can make the ray appear to come from outside the $\pm$ 36° shadow cone, specifically, at an angle of 90°-45° = 45°. For lower TKR frequencies the angle of deviation is greater, while for higher frequencies it is less. Thus it is of interest to determine what fraction of the large angle events might be due to wake refraction rather than scattering. Since the wake is aligned in the anti-sunward direction, RAE-2 must pass through some portion of the wake during an occultation of the sun, and this occurred on only 18 of our 80 events (23%). Scattering events which are observed from dayside local time positions of the moon between about 0400-2000 hours will not be affected by wake refraction since the spacecraft does not cross the wake during the occultation. The high inclination (60°) and precession of the RAE-2 orbital plane also means that even in the nightside local time range of 2000-0400 hours including the magnetosheath some earth occultations will occur during which the spacecraft will not enter the wake. Thus, the effects of lunar wake refraction tend to be minimized and do not substantially reduce the number of true scattering events.

CONCLUSIONS

In the preceding section, we have presented arguments in favor of an explanation of the observation of TKR during deep Earth occultations that is based on propagation effects rather than on the actual generation of the emission at very large geocentric distances. Two alternative scattering mechanisms appear to be plausible. In the first, we would expect strong scattering or irregular refraction to be occurring in the magnetosheath due to large scale density inhomogeneities characterized by electron density fluctuations, $\Delta N/N$, of $\sim 50\%$ and scale sizes of less than a few R_E. In the second alternative, we expect large angle Bragg scattering off ion plasma waves in the magnetosheath and/or the solar wind which have wavelengths that are nearly equal to the incident TKR wavelengths. At the present time, we cannot determine which alternative mechanism is more important; they probably both contribute at different times. There is already observational evidence that both the macroscale structure and the microscale features required to produce the scattering do occur in the region of the magnetosheath. New information which will come from experiments on the ISEE-1 and 2 spacecraft should provide a more detailed assessment of the existence of the scatterers we propose.

The interpretation of the very distant kilometric emissions in terms of strong scattering effects has broader implications which may help to resolve a number of questions about the locations of the radio source(s). In our earlier studies of the source positions (e.g., Kaiser and Alexander, 1976; Alexander and Kaiser, 1976) we found that most strong

TKR emissions were observed to originate from within a geocentric distance of 4 R_E, but that there were still a significant number of occassions when source components were observed at greater distances. Some of the more distant source position results could quite possibly be due to the same magnetosheath scattering effects that we have discussed above to explain the extreme lunar occultation events.

On the other hand, a number of the TKR source components observed at radial distances of ~ 5 to 15 R_E appear to be aligned along a specific family of geomagnetic field lines or flux tube. This effect is not likely to be a consequence of scattering in the magnetosheath, but the apparent source configuration might be due to discrete scattering regions which are constrained to a limited region in the magnetosphere. Indeed, the possibility of some special propagation effect as the explanation for the apparent occurrence of TKR at large distances was suggested when we first reported the lunar occultation results (D. Gurnett, private communication), and we have noted in an earlier paper (Kaiser and Alexander, 1977a) that the plasma wave turbulence observed on auroral field lines by Gurnett and Frank (1977) may provide the necessary field-aligned scattering centers. The present analysis tends to reinforce that hypothesis.

We conclude this discussion with a retrospective summary of the present picture of the TKR source regions. Most of the emission is apparently generated inside of 5 R_E with a geocentric radial distance of ~ 2 R_E being our present best estimate for the most commonly occurring location. Determination of source size is limited by the time resolution of the RAE-2 lunar occultation measurements, by diffraction effects at the lunar limb, and by scattering. We can place an upper limit on the

typical source dimensions of 1 R_E. We do not completely rule out the occurrence of kilometric radio sources at distances of greater than ~ 5 R_E or over areas of several R_E^2 (such as a portion of the magnetosheath), but their radiated power levels and their frequency of occurrence are probably much lower than the intense, lower altitude, auroral kilometric radiation sources commonly observed during magnetospheric substorms.

ACKNOWLEDGEMENTS

We are grateful to our colleagues L. F. Burlaga, D. H. Fairfield and J. Hornstein for a number of useful comments and suggestions. Much of the preparation and reduction of the RAE data was done by Mrs. P. Harper and Mrs. S. Vaughan to whom we owe special thanks.

REFERENCES

Alexander, J. K., and M. L. Kaiser, Terrestrial kilometric radiation, 1, Spatial structure studies, J. Geophys. Res., 81, 5948, 1976.

Alexander, J. K., and M. L. Kaiser, Terrestrial kilometric radiation, 2, Emission from the magnetospheric cusp and dayside magnetosheath, J. Geophys. Res., 82, 98, 1977.

Bekefi, G., Radiation Processes in Plasmas, John Wiley and Sons, New York, 1966.

Chandasekhar, S., A statistical basis for the theory of stellar scintillation, Mon. Not. Roy. Ast. Soc., 112, 475, 1952.

Fairfield, D. H., Average and unusual locations of the Earth's magnetopause and bow shock, J. Geophys. Res., 76, 6700, 1971.

Farley, D. T., Radio wave scattering from the ionosphere, in Methods of Experimental Physics, 9B, edited by R. H. Lovberg and H. R. Griem, p. 139, Academic Press, New York, 1971.

Gosling, J. T., E. Hildner, J. R. Asbridge, S. J. Bame, and W. C. Feldman, Noncompressive density enhancements in the solar wind, J. Geophys. Res., 82, 5005, 1977.

Greenstadt, E. W., Phenomenology of the Earth's bow shock system. A summary description of experimental results, in Magnetospheric Particles and Fields, edited by B. M. McCormac, p.13, D. Reidel, Dordrecht-Holland, 1976.

Gurnett, D. A., The Earth as a radio source: The nonthermal continuum, J. Geophys. Res., 80, 2751, 1975.

Gurnett, D. A., and L. A. Frank, A region of intense plasma wave turbulence on auroral field lines, J. Geophys. Res., 82, 1031, 1977.

Gurnett, D. A., and L. A. Frank, Ion acoustic waves in the solar wind, J. Geophys. Res., 83, 58, 1978.

Hamberger, S. M., and J. Jancarik, Experimental studies of electrostatic fluctuations in the turbulently heated plasma, Phys. Fluids, 15, 825, 1972.

Howe, H. C., and J. H. Binsack, Explorer 33 and 35 plasma observations of magnetosheath flow, J. Geophys. Res., 77, 3334, 1972.

Kaiser, M. L., and J. K. Alexander, Source location measurements of terrestrial kilometric radiation obtained from lunar orbit, Geophys. Res. Lett., 3, 37, 1976.

Kaiser, M. L., and J. K. Alexander, Terrestrial kilometric radiation, 3, Average spectral properties, J. Geophys. Res., 82, 3273, 1977a.

Kaiser, M. L., and J. K. Alexander, Relationship between auroral substorms and the occurrence of terrestrial kilometric radiation, J. Geophys. Res., 82, 5283, 1977b.

Kaufmann, R. L., and J.-T. Horng, Physical structure of hydromagnetic disturbances in the inner magnetosheath, J. Geophys. Res., 76, 8189, 1971.

King, J. H., Interplanetary medium data book, National Space Science Data Center/World Data Center A for Rockets and Satellites publication 77-04, 1977.

Kurth, W. A., M.M. Baumback, and D.A. Gurnett, Direction finding measurements of auroral kilometric radiation, J. Geophys. Res., 80, 2764, 1975.

Ness, N.F., K.W. Behannon, H.E. Taylor and Y.C. Whang, Perturbations of the interplanetary magnetic field by the lunar wake, J. Geophys. Res., 73, 3421, 1968.

Rodriguez, P., and D.A. Gurnett, Electrostatic and electromagnetic turbulence associated with the Earth's bow shock, J. Geophys. Res., 80, 19, 1975.

Rodriguez, P., Magnetosheath electrostatic turbulence, to appear in J. Geophys. Res., 1978a.

Rodriguez, P., Ion waves associated with solar wind beam-plasma interactions, (in prep), 1978b.

Sheffield, J., Plasma Scattering of Electromagnetic Radiation, Academic Press, New York, 1975.

Spreiter, J. R., and A. W. Rizzi, Aligned magnetohydrodynamic solution for solar wind flow past the Earth's magnetosphere, Acta Astronautica, 1, 15, 1974.

Vesecky, J. F., and M. S. Frankel, Observations of a low-frequency cutoff in magnetospheric radio noise received on IMP 6, J. Geophys. Res., 80, 2771, 1975.

Voots, G. R., D. A. Gurnett and S.-I. Akasofu, Auroral kilometric radiation as an indicator of auroral magnetic disturbances, J. Geophys. Res., 82, 2259, 1977.

West, H. I., Jr., and R. M. Buck, Observations of > 100 kev protons in the Earth's magnetosheath, J. Geophys. Res., 81, 569, 1976.

Whang, Y.C., Field and plasma in the lunar wake, Phys. Rev., 186, 143, 1969.

FIGURE CAPTIONS

Figure 1 Examples of dynamic spectra obtained from RAE-2 during deep lunar occultations of the Earth. Each strip displays the variation of received signal level (with darkness proportional to intensity) between 0.025 and 13.1 MHz over a 100-min span of time. The period of lunar occultation of the Earth's surface is denoted by the arrows.

Figure 2 Plots of projections of the moon's limb (right-hand panels) and power flux density spectra (left-hand panels) for two examples of RAE-2 reception of kilometric radiation from large angular distances from the Earth. The right-hand panels show the projection of the moon's limb onto a plane through the Earth perpendicular to the line of sight from RAE-2 to the Earth at 10-min. intervals of U.T. The left-hand panels display the average flux spectrum observed at kilometric wavelengths during the 10-min. interval that included the deepest part of the occultation. L. T. is the sub-lunar local time at the Earth at the time of the occultation.

Figure 3 Ecliptic plane projections of the region blocked by the moon (shaded area) during central occultations of the Earth that were not accompanied by an interuption of reception of TKR at RAE-2. The heavy dot shows the location of the satellite in lunar orbit with respect to nominal bow shock and magnetopause locations.

Figure 4 Inferred directions of arrival of TKR during a number of deep ($> 10^{o}$) lunar occultations of the Earth. Each arrow is drawn from the location of RAE-2 in lunar orbit toward the apparent source direction rotated into the ecliptic plane. A nominal bow shock and magnetopause location (Fairfield, 1971) are shown for reference.

Figure 5 Plot of the variation of the frequency of peak TKR power flux density, f_o, during deep lunar occultation events versus the hourly average solar wind electron plasma frequency, $f_{p(sw)}$, for the occultation period.

Figure 6 (a) The average power pattern of 110 kHz TKR as a function of the observer's sub-satellite local time. (b) The minimum path length through the average magnetosheath to the Earth for an observer in lunar orbit. (c) The normalized product of the distributions shown in (a) and (b). (d) The observed occurrence probability pattern for RAE-2 detection of TKR during deep lunar occultations.

Figure 7 A model for the observation of TKR scattered from the solar wind and/or magnetosheath during a central lunar occultation. The shadow zone, indicated by the shading, should be viewed as a three-dimensional cone. TKR rays which are incident (i) on a scattering center (plasma waves) with the appropriate wavelength become scattered rays (s) at an angle θ, and thus appear to come from outside the shadow zone. The boundary locations for

plasma wave turbulence are variable, depending on the orientation of the magnetic field.

Figure 8 The Bragg scattering relation, showing that for large angle scattering ($\theta \gtrsim 60^{o}$) of incident TKR wavelengths λ_i, the wavelengths λ of the scattering centers must be (1-2)km. The shaded intervals on the vertical axis give the range of values of λ/λ_i for selected values of λ

Figure 1

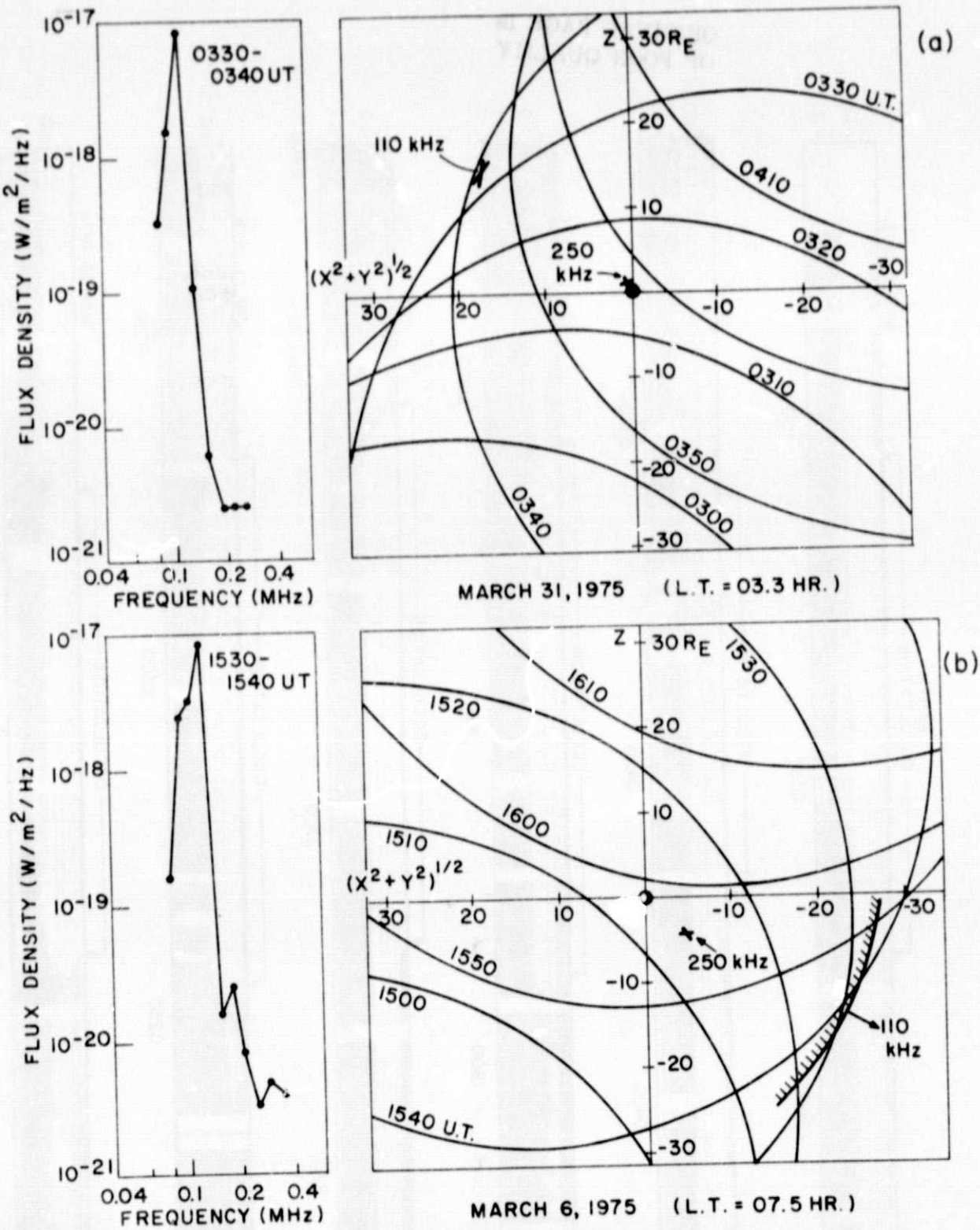
FLUX DENSITY (W/m²/Hz)
10⁻¹⁷
10⁻¹⁸
10⁻¹⁹
10⁻²⁰
10⁻²¹
0330-
0340 UT
0.04 0.1 0.2 0.4
FREQUENCY (MHz)
Z = 30 R_E
(a)
0330 U.T.
110 kHz
0410
20
10
0320
-30
250
kHz
(X²+Y²)^1/2
30 20 10 -10 -20
-10
0310
0350
-20
0300
0340
-30
MARCH 31, 1975 (L.T. = 03.3 HR.)
FLUX DENSITY (W/m²/Hz)
10⁻¹⁷
10⁻¹⁸
10⁻¹⁹
10⁻²⁰
10⁻²¹
1530-
1540 UT
0.04 0.1 0.2 0.4
FREQUENCY (MHz)
Z = 30 R_E
1530
(b)
1610
1520
20
1600
10
1510
(X²+Y²)^1/2
30 20 10 -10 -20 -30
250 kHz
1550
-10
1500
110
kHz
-20
1540 U.T.
-30
MARCH 6, 1975 (L.T. = 07.5 HR.)

Figure 2

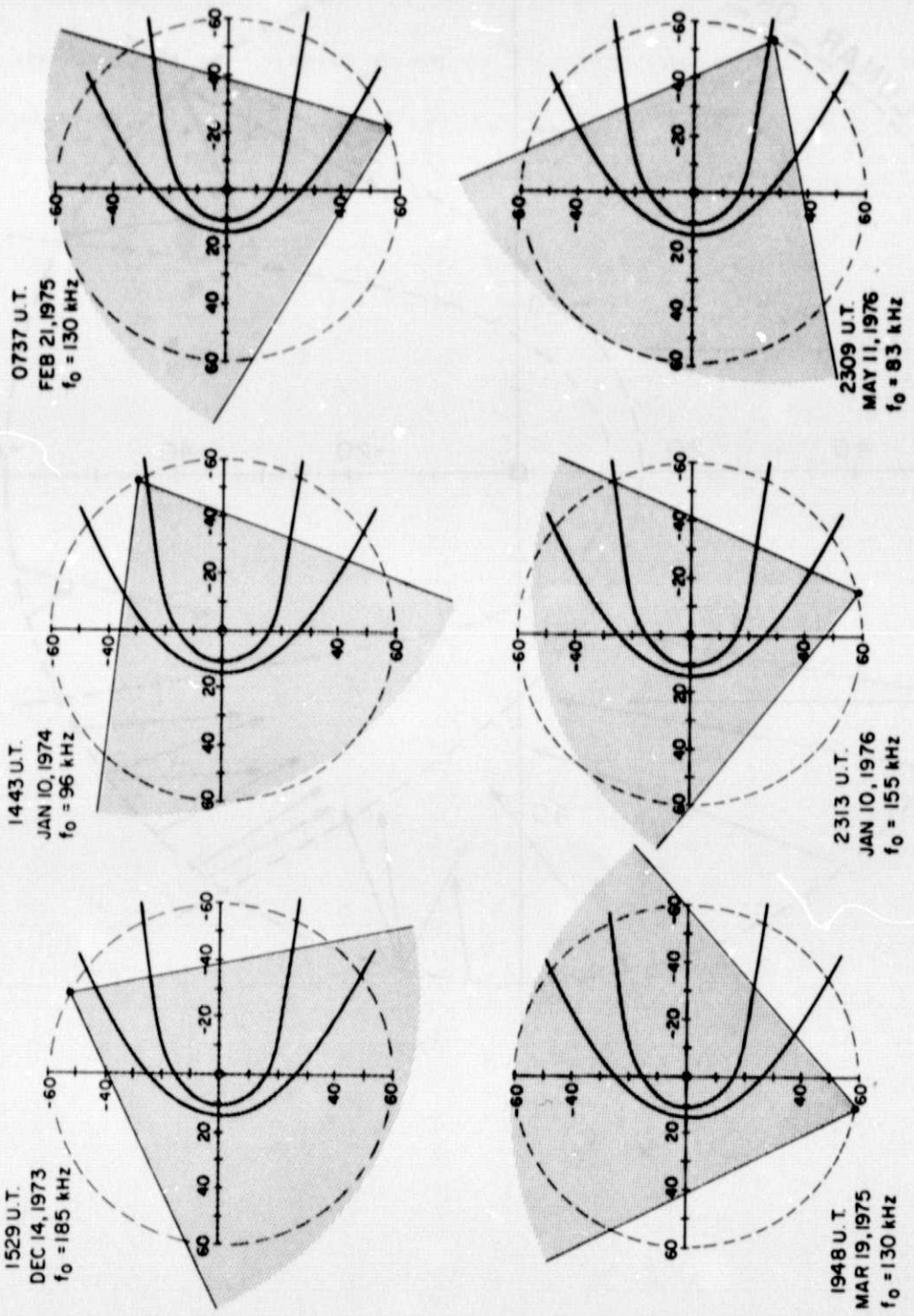

Figure 3

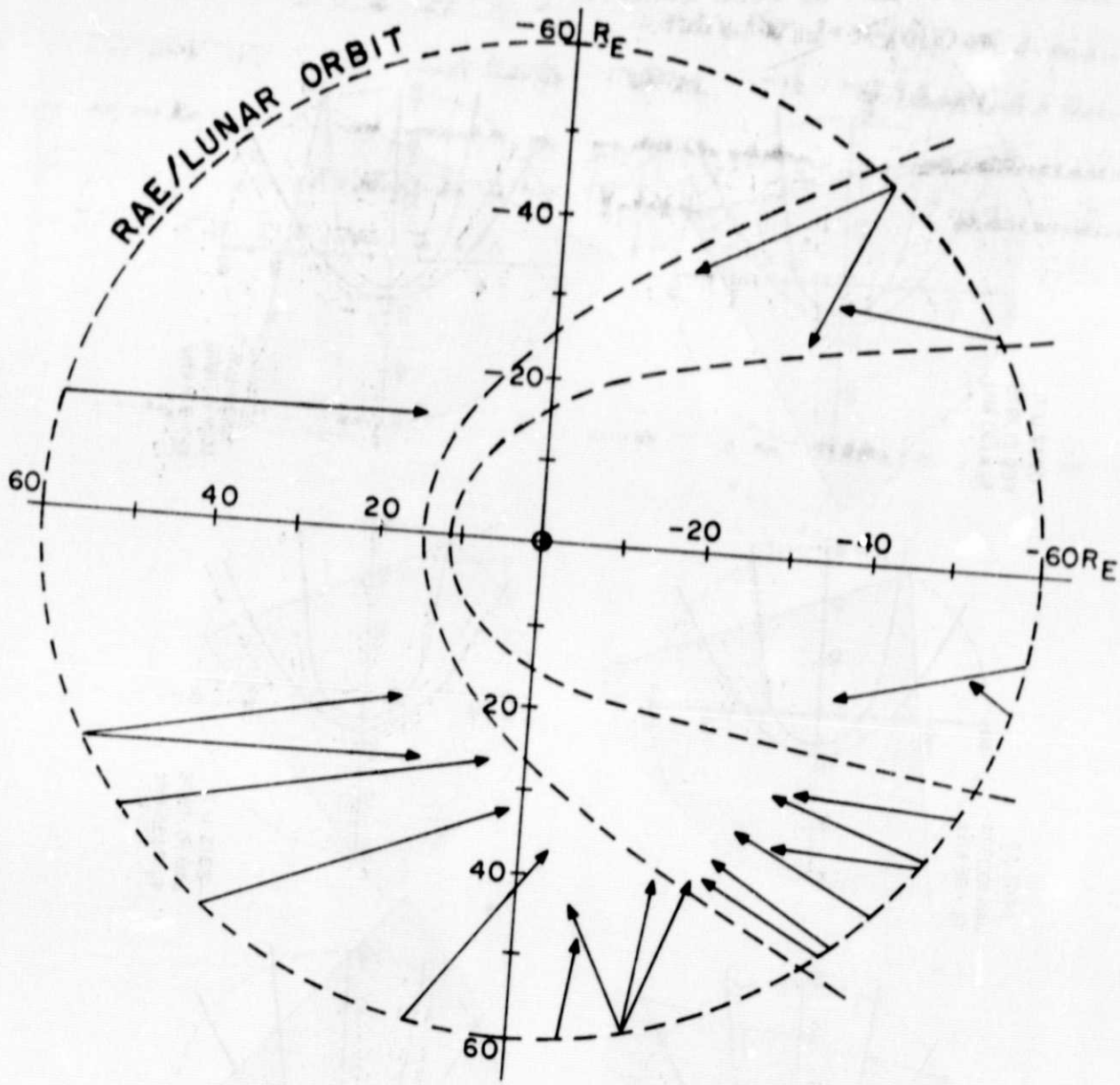

Figure 4

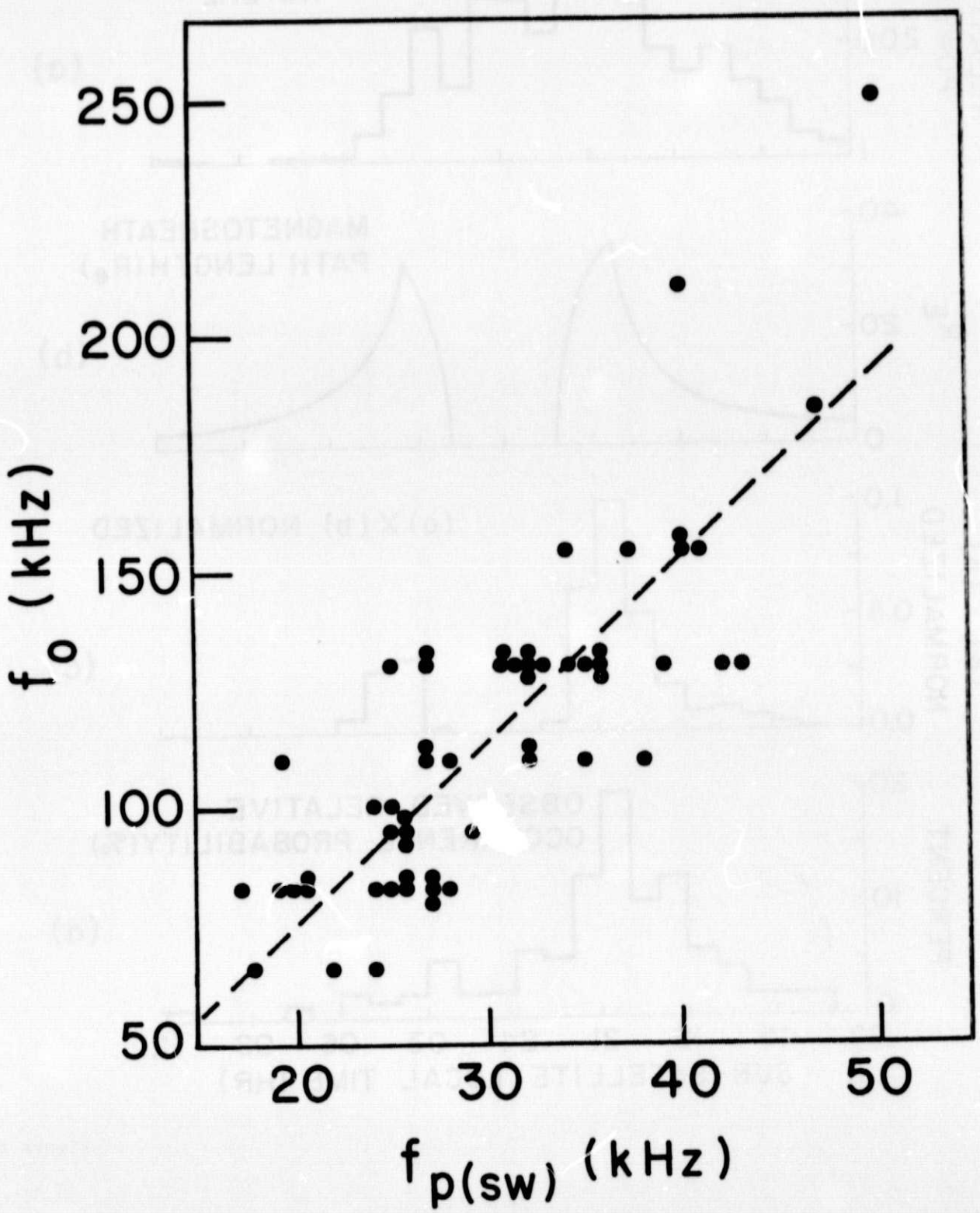

Figure 5

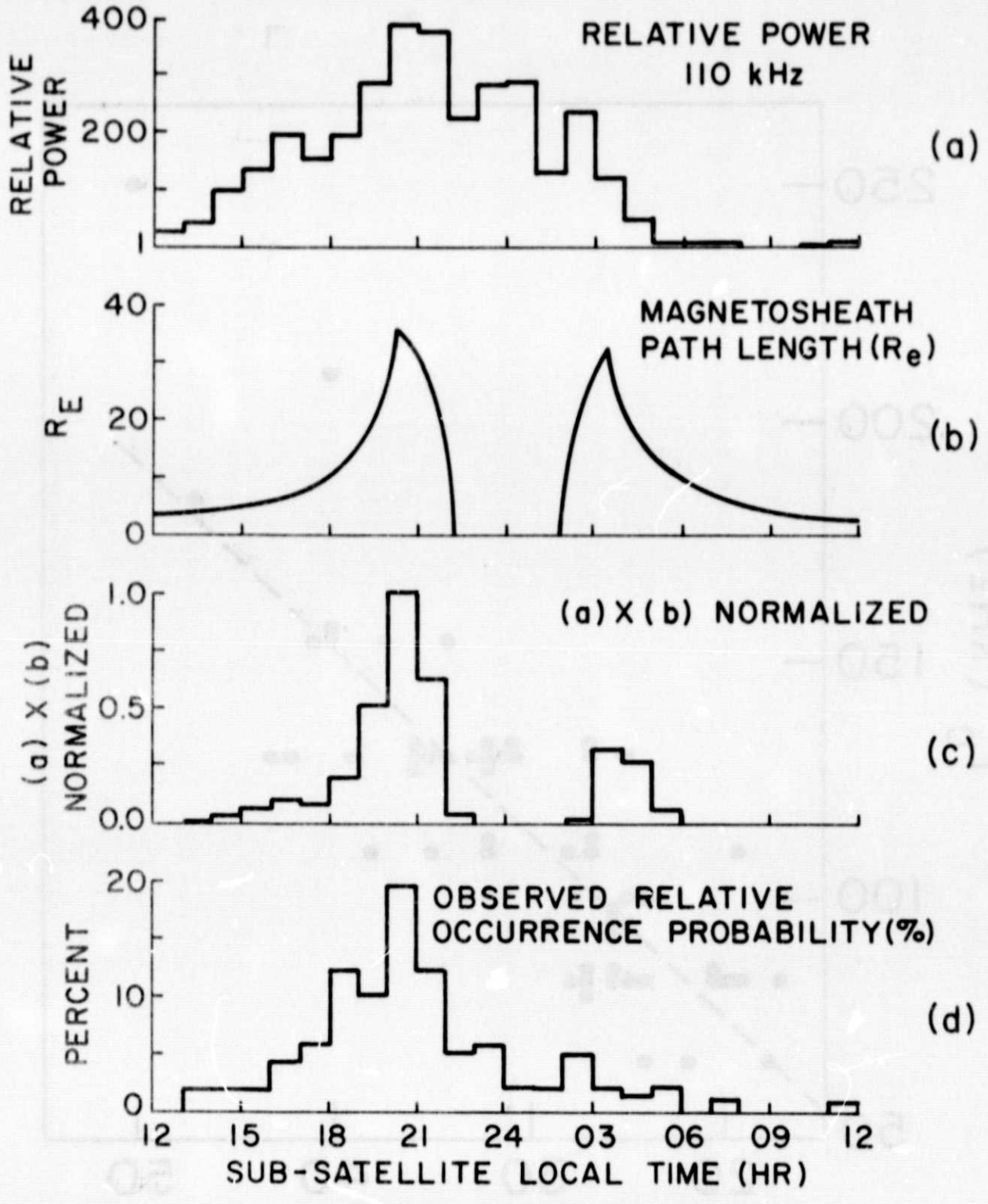
RELATIVE POWER
400
200
1
RELATIVE POWER
110 kHz
(a)
40
20
0
R_E
MAGNETOSHEATH
PATH LENGTH (R_e)
(b)
1.0
0.5
0.0
(a) X (b) NORMALIZED
(a) X (b) NORMALIZED
(c)
20
10
0
PERCENT
OBSERVED RELATIVE
OCCURRENCE PROBABILITY (%)
(d)
12 15 18 21 24 03 06 09 12
SUB-SATELLITE LOCAL TIME (HR)

Figure 6

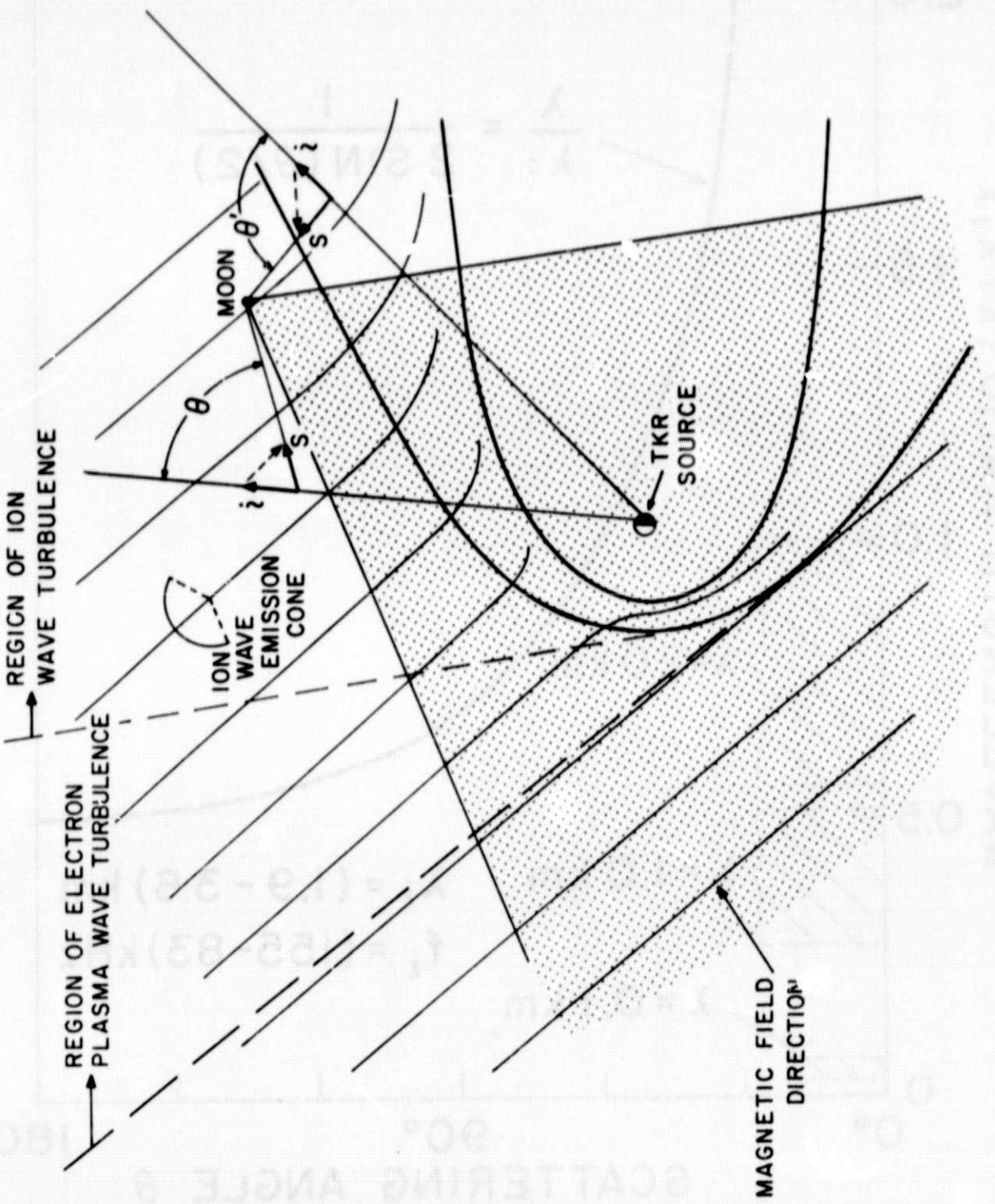

Figure 7

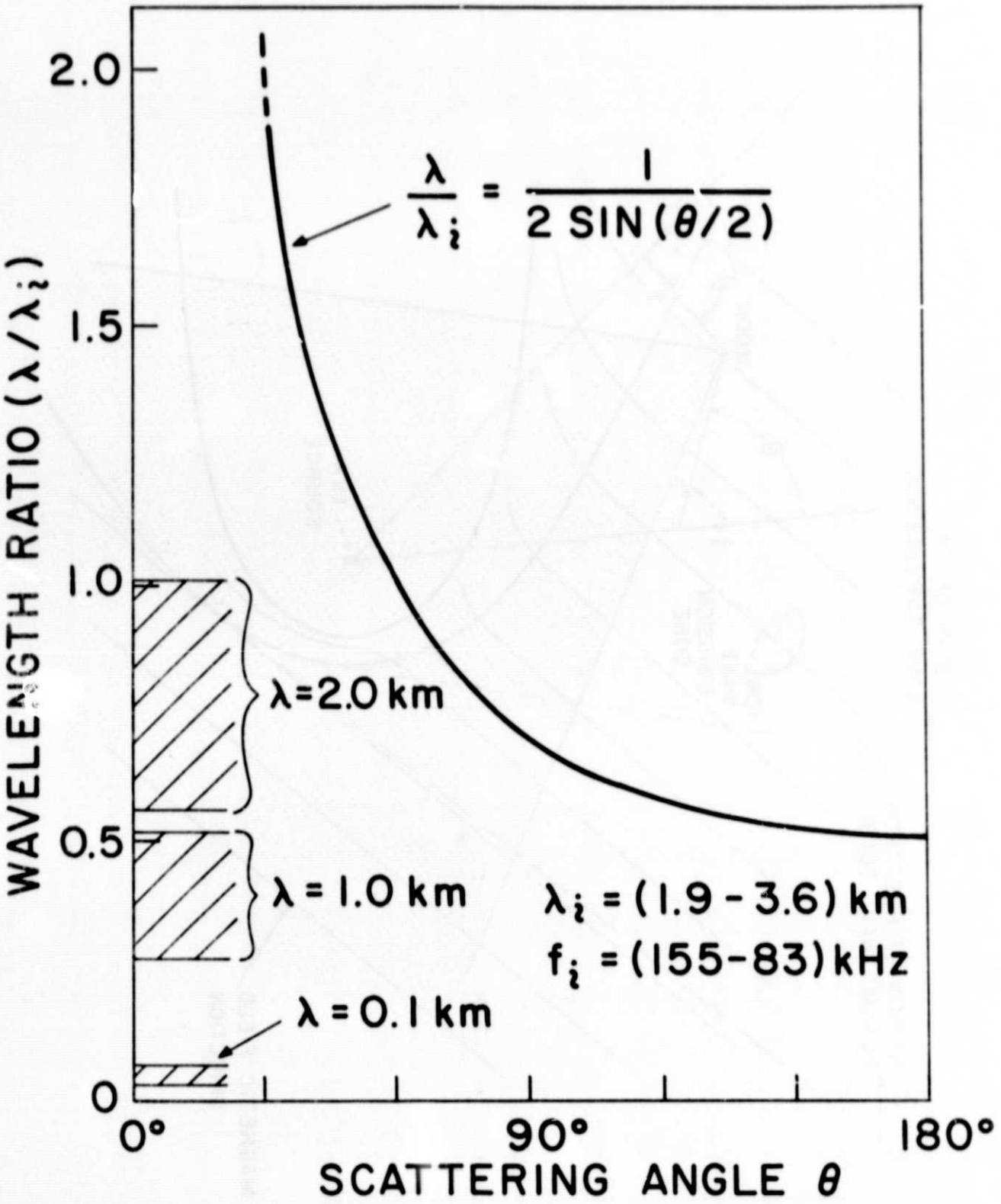
2.0
1.5
1.0
0.5
0
WAVELENGTH RATIO (λ/λi)
λ/λi = 1 / 2 SIN(θ/2)
λ=2.0 km
λ = 1.0 km
λ = 0.1 km
λi = (1.9 - 3.6) km
fi = (155-83) kHz
0°
90°
180°
SCATTERING ANGLE θ

Figure 8